Syndiotactic Polystyrene Preparation in a Rim Process

T. M. LIU, W. E. BAKER,* VIVI SCHYTT,† TODD JONES,‡ and M. C. BAIRD

Department of Chemistry, Queen's University, Kingston, Canada, K7L 3N6

SYNOPSIS

Very few polymeric systems are suitable for preparing engineering parts using reaction injection molding (RIM) processing. A new two-component metallocene catalyst, which is able to polymerize bulk styrene at high rates to the syndiotactic form, was studied. The catalyst used in this work was based on monocyclopentadienyl analogs of titanium (Cp^*TiMe_3), which was used in conjunction with a boron cocatalyst [$B(C_6F_5)_3$]. When separate streams of the catalyst and cocatalyst, dissolved in either styrene or styrene/toluene solutions, met in a mixhead, the styrene polymerized rapidly to form crystalline, syndiotactic polystyrene (s-PS). Using a bench scale RIM device, the monomer conversion during polymerization was monitored through the quasi-adiabatic temperature rise, recorded by a rapid data acquisition system. The rate equation was found to be second order with respect to the monomer concentration and first order with respect to the catalyst concentration, given some assumptions. The s-PS was brittle and attempts were made to incorporate elastomer toughening into the reacting system. Several potential problems associated with using this system for RIM process are discussed. © 1996 John Wiley & Sons, Inc.

INTRODUCTION

Atactic polystyrene (a-PS) is one of the four major commodity polymers widely used in the world today because of its low cost and easy processability. However, a-PS has inferior thermal properties, since it is unable to crystallize and has a glass transition at approximately 100°C. In 1986, Ishihara et al.[1] showed that it was possible to produce syndiotactic polystyrene (s-PS) at room temperature using a new family of extremely active catalysts, commonly known as metallocene catalysts. Work has continued on developing these catalysts, since s-PS has the ability to crystallize and is highly resistant to solvents. The crystalline melting point of s-PS is 260–270°C, which offers the potential for improving the high-temperature properties of PS. Initial studies[2] demonstrated that the dynamic mechanical and thermal properties of s-PS are similar to those of poly(ethylene terephthalate); therefore, s-PS is a potential engineering polymer candidate.

Recently, a new metallocene catalyst system having the ability to generate highly stereoregular s-PS was developed.[3,4] This system, composed of a pentamethylcyclopentadienyltrimethyl titanium (Cp^*TiMe_3) catalyst and a tris-(pentafluorophenyl)borane [$B(C_6F_5)_3$] stabilizing cocatalyst, was capable of producing high molecular weight ($>10^5$) s-PS with a narrow molecular weight distribution ($M_w/M_n \approx 2$). The s-PS produced by this reaction formed a solid plug in a test tube. The polymer appeared to solidify within 120 s of the reaction's initiation, which is much faster than the 2 h reaction time required with the Ishihara catalyst system. It was felt that this catalyst system might allow s-PS to be used in reaction injection molding (RIM),[5] a method of polymer processing possessing a number of distinct advantages, compared to traditional methods of forming polymers. These advantages include lower mold pressures and mold temperatures, the ability to form large and complex parts, and the potential for long-strand composite reinforcement. In the past, RIM has been limited in its application, being based on a very limited number of polymer systems such as polyurethanes and polyureas. If the use of a commodity monomer such as styrene

* To whom correspondence should be addressed.
† Present address: Institut for Kemiteknik, Denmark.
‡ Present address: University of Minnesota, MN.

Journal of Applied Polymer Science, Vol. 62, 1807–1818 (1996)
 CCC 0021-8995/96/111807-12

could be perfected, RIM processing could gain much wider use.

Lipshitz and Macosko[6] pointed out that to model RIM processing a basic knowledge of the reaction kinetics is important. However, kinetic studies involving extremely high monomer concentrations or bulk conditions using this particular metallocene system [Cp*$TiMe_3$)/($B(C_6F_5)_3$] are not known. Much of the literature concentrates on the methylaluminoxide cocatalyst system and does not, in general, provide any kinetic information. The objective of this project was to construct a system suitable for studying the potential of this catalyst/cocatalyst system for use in RIM conditions. The kinetics of the polymerization of styrene to the s-PS using this system were examined under conditions appropriate for reaction molding.

The s-PS produced in this process has the usual brittleness of atactic polystyrene at room temperature. The RIM process suffers from the shortcoming that the molded product must have all the requisite properties developed in the one-step molding process from monomers. No subsequent modification process is possible. Hence, this process appears to have little merit if s-PS cannot be toughened *in situ* in the RIM process. Furthermore, whatever toughening mechanism is used, it cannot interfere with the sensitive catalyst. Hence, a number of trials were carried out in which different elastomers were incorporated into the reacting system.

EXPERIMENTAL

A simplified method of RIM was used to polymerize styrene to the syndiotactic form in the presence of toluene, using the metallocene catalyst/cocatalyst system described above. The reaction temperature was monitored and used as an indication of monomer conversion.

Equipment

Since the catalyst and cocatalyst are both extremely sensitive to moisture and oxygen, the RIM apparatus was contained in a dry box, under a nitrogen atmosphere (see Fig. 1). Delivery of the two liquid components was accomplished using 10 cc BDH syringes, attached to shortened needles. These were connected to the mixhead assembly by $\frac{1}{8}$ in. inside diameter Fisher brand PVC clear tubing.

The mixhead itself (see Fig. 2) was constructed of standard laboratory glass tubing. To maximize mixing, two contributing steps were employed: impingement mixing, by directing the two incoming streams directly at each other, resulting in an intimate contact of the liquids; and static mixing, by passing the resulting fluid through a Kenics static mixer. In considering the effectiveness of mixing by impingement, a quantitative assessment of the Reynolds number (R_e) is essential. The Reynolds number is given by

Experimental Apparatus

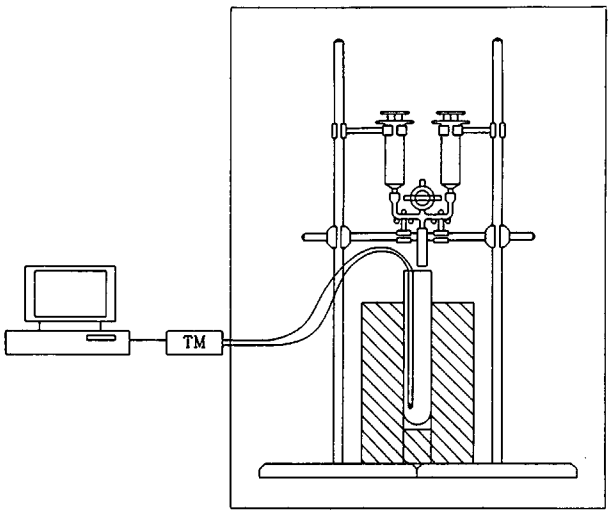

Figure 1 The miniature laboratory RIM device.

$$R_e = \frac{4\rho Q}{\pi \eta d} \quad (1)$$

including the following terms: flow rate (Q), density (ρ), viscosity (η), and diameter (d). Macosko noted that a value of $R_e > 500$ is required for good mixing by impingement.[5] Based on a fluid delivery rate of 1 mL/s, the inlet tubes were chosen to have an inside diameter of 1 mm, as this gives $R_e > 5000$ for both components, which is far above the required minimum. The eight element $\frac{3}{16}$ in. polypropylene Kenics mixers, supplied by Cole-Parmer, were contained inside Nalgene semirigid polyethylene tubing. This assembly was connected to the mixhead by heating and fitting the tubing over the impingement mixing outlet, as shown in Figure 2, thereby preventing leakage at the joint. This also allowed the static mixer assembly to be easily discarded and replaced if solidification of the reaction mixture occurred inside the mixer.

The mixhead outlet fed directly into a 25 mL glass test tube. A disposable type T (copper-constantan) thermocouple, having a response time of 1.1 s, was used.[7] The thermocouple bead was suspended in the

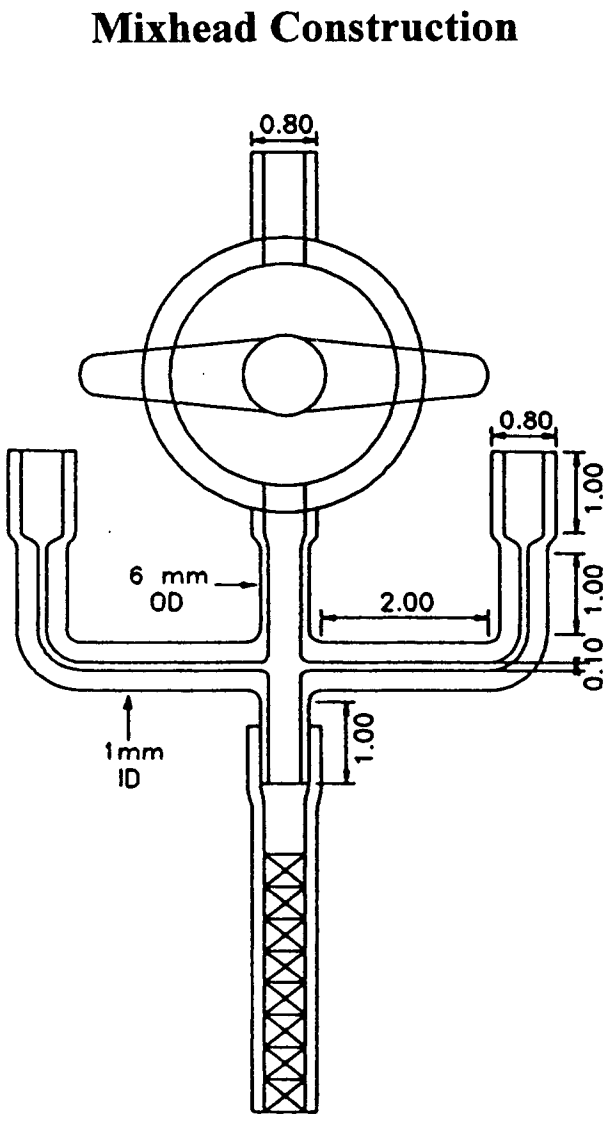

Figure 2 RIM mixhead construction. All dimensions in cm, except where indicated. Material of construction is standard glass, except the Kenics mixer (PP) and surrounding tubing (semirigid PE).

center of the base of the test tube. The thermocouple signal was fed to an Omega Engineering DP-41 temperature meter with a serial communications board connected to a personal computer, running a simple data acquisition program written in BASIC.

The RIM apparatus was assembled using four clamps to attach the mixhead and syringes to retort stands, as shown in Figure 1. The clamps connected to the syringes bore the force exerted during liquid delivery to the mixhead, while those supporting the mixhead ensured correct positioning. To achieve equal rates of delivery, a common steel handle was used.

This apparatus allowed for intimate mixing of the liquid components, convenient disassembly and cleaning, accurate metering of the two components at equal flow rates, and easy disposing of the mixing unit and temperature monitoring system. It did, however, require that the two equal volumes of fluid have the appropriate stoichiometric ratio of catalyst and cocatalyst.

Materials

Styrene commercially available from Aldrich was purified and dried. The styrene was stripped of its inhibitor (4-*tert*-butylcatechol) by passing through an inhibitor removal column. To remove air, the styrene was repeatedly frozen in liquid nitrogen under a vacuum and thereafter thawed under vacuum. Furthermore, molecular sieves were added to the styrene to avoid moisture retention.

Standard reagent-grade toluene was dried with sodium and benzophenone and distilled under an atmosphere of nitrogen. The high-purity catalyst Cp^*TiMe_3 and cocatalyst $B(C_6F_5)_3$ were prepared as described earlier and stored in a freezer under an atmosphere of nitrogen.[3] Four types of thermoplastic rubbers and two types of core–shell rubber tougheners in powder form were obtained commercially and are listed in Table I.

Polymerization

The catalyst was dissolved in a prescribed volume of purified and dried styrene. The solution was then drawn into a syringe and attached to the mixhead. An appropriate quantity of cocatalyst was dissolved in toluene or in a mixture of toluene and styrene to study the effect of monomer concentration on the reaction. An equivalent volume of this cocatalyst solution was drawn into the second syringe and attached to the mixhead. The initial monomer and the catalyst concentrations are summarized in Table II. The molar ratio of catalyst to cocatalyst was 1. The two syringes were depressed uniformly to obtain even contact of the two streams in the mixhead, down through the mixer, and into the test tube. The total injection time was 3–4 s. A very hard, dark solid, retaining the shape of the test tube, was formed within 15–120 s, depending on the starting conditions. The reaction product was removed from the test tube after 10 min and prepared for characterization. Purification of the resulting polymer, to remove the entrained catalyst, was accomplished by dissolving the polymer in 1,2,4-trichlorobenzene at 140°C, followed by precipitation in 1% HCl in

Table I Rubbers Tested as Toughening Modifier

Product Identification	Manufacture	Chemical Description
Kraton D 1101	Shell Co.	Linear styrene–butadiene–styrene (SBS) triblock copolymer
Kraton D 1102	Shell Co.	Linear styrene–butadiene–styrene (SBS) triblock copolymer
Kraton D 1107	Shell Co.	Linear styrene–isoprene–styrene (SIS) triblock copolymer
Kraton G 1652	Shell Co.	Linear styrene–ethylene/butylene–styrene (SEBS) block copolymer
Paraloid EXL 2300	Rohm and Haas Co.	Acrylic impact modifier powder form (0.35 micron)
Paraloid EXL 2691	Rohm and Haas Co.	Methacrylate/butadiene/styrene (MBS) impact modifier

methanol. The precipitates were then washed three times with 50 mL aliquots of methanol and dried in a vacuum at 90°C to constant weight. Chein and Salajka[8] measured the content of a-PS in s-PS using an extraction technique with refluxing 2-butanone for 4 h. In our experiment, Soxhlet extraction with acetone was performed to remove the a-PS fraction (soluble). The percentage of a-PS was determined using a mass balance on the dried polymer before and after the extraction. The insoluble fractions were identified using DSC and ^{1}H-NMR.

Characterization

Thermal Analysis

Differential scanning calorimetry (DSC) analysis was performed on a Mettler TA 3000 DSC equipped with a Mettler TC 10A data processor. The heating scan rate was 10°C/min. The temperature and heat flow scales were calibrated using high-purity indium and zinc samples.

Table II The Initial Monomer Concentration and the Catalyst Concentration for Polymerization of s-PS

No. Recipe	Catalyst Concn. (mol/L)	Monomer Concn. (mol/L)
1	0.0075	7.61
2	0.010	7.61
3	0.015	7.61
4	0.015	6.52
5	0.015	4.35
6	0.015	2.17
7	0.020	7.61

Thermogravimetric analysis (TGA) was carried out using a Mettler TA 3000 system with a TG 50 thermobalance. The temperature scan rate was 10°C/min over a range from 30 to 500°C. The crucible was filled with a known weight of experimental sample (about 10 mg).

^{1}H-Nuclear Magnetic Resonance

^{1}H-NMR was used to substantiate the presence of s-PS. The spectra were acquired using a Bruker AM 400 MHz spectrometer. NMR samples were prepared by dissolving 20 mg of an acetone-insoluble fraction into 0.5 mL of CD_2Cl_2. Samples were heated at 120°C for 2 h prior to analysis to completely dissolve the polymer.

High-temperature GPC

The molecular weight of the s-PS samples was determined using a Waters Associates Model 150C ALC/GPC chromatograph at 145°C. The GPC was calibrated using PS standards. 1,2,4-Trichlorobenzene (TCB) was used as the carrier fluid, and the flow rate was 1 mL/min. Four blank samples were run to stabilize the base line.

RESULTS AND DISCUSSION

The thermal traces of the acetone-insoluble fraction are shown in Figure 3. The top DSC trace is representative of the PS that is formed in the RIM apparatus. The sample shows a glass transition point at 95°C and melts at 274°C. The bottom trace is for the same sample but after quenching from 300°C to 25°C at a cooling rate of 360°C/min. The glass

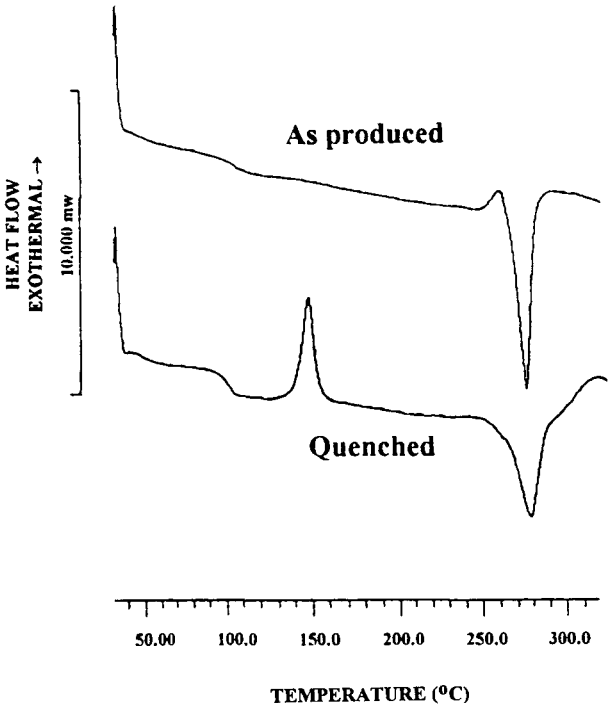

Figure 3 DSC traces of the acetone-insoluble PS.

transition is more prominent while the melting endothermic peak decreases. There is also a new exothermic peak at 148°C, which arises from the cold crystallization of the quenched sample. The ^{1}H-NMR spectrum of the methine and methylene protons of the sample is shown in Figure 4. These data are similar to that reported by Ishihara et al.[1] The triplet at $\delta = 1.45$ ppm is assigned to the methylene proton and suggests that the two methylene protons of the PS sample are equivalent, indicating that the structure of this PS sample is syndiotactic. The results from these studies confirm that the PS formed in our system is s-PS.

The top DSC trace in Figure 3 was employed to measure the fractional crystallinity (X_c) of the samples:

$$X_c = \Delta H_m / \Delta H_m^0 \qquad (2)$$

where ΔH_m is the heat absorbed during melting and ΔH_m^0 (= 53 mJ/mg) is the theoretical heat absorbed during melting for fully crystalline samples.[9]

The properties of the PS synthesized in this work are summarized in Table III. The observed melting temperature for these samples ranges from 270 to 274°C, which is higher than the melting point (~ 240°C) of isotactic PS. The glass transition temperature is around 95°C and is close to the T_g of a-PS and isotactic PS. The crystallinity of the samples is between 10 to 15%, while the M_w is relatively high ($0.39–0.69 \times 10^6$) and the polydispersity is low (1.50–1.98). The acetone-insoluble part is over 90%.

Conversion Studies

The final monomer conversion was calculated for each recipe using a mass balance on the starting monomer and the total polymer produced, and the results are shown in column two of Table IV. To validate this technique of using a mass balance to determine conversion, TGA was performed on the same samples. A typical TGA trace for these runs is shown in Figure 5. The weight of the sample vs. temperature is given in Figure 5(a), and the derivative of weight over time (DTG) is shown in Figure 5(b). Three peaks were observed at 100, 142, and 415°C. The first two peaks overlapped significantly and were resolved by partitioning the area of the total peak at 115°C. Since at atmospheric pressure toluene has a boiling point of 110.6°C and styrene has a boiling point at 145.2°C,[10] peaks 1 and 2 were assigned to these two components, respectively. The third peak was assigned to the thermodegradation of PS. After separating the solvent peaks into the respective toluene and styrene fractions, the conversion for each recipe was calculated and is given in column three of Table IV. The results confirmed that the final monomer conversion as measured by TGA was in agreement with the mass balance method.

The temperature in the reaction mass was recorded as a function of time and allowed to rise up to a constant value, indicating, essentially, the end of the reaction. A typical temperature vs. time trace is shown in Figure 6. The solidification time was determined qualitatively, by visually observing the movement of the reaction mixture on gentle shaking. Solidification occurred within 15–120 s of mixing, depending on the starting conditions of the reaction. The system in Figure 6 began to solidify at about 110 s. The reacting components were still low viscosity liquids when entering the test tube.

Correction for Heat Loss

Lipshitz and Macosko[6] pointed out that due to the fast reaction times commonly associated with RIM system conventional methods of monitoring conversion have not, in general, been applicable. A method of monitoring the monomer conversion, through the adiabatic temperature rise in a fast polymerizing system, has been developed; thus, kinetic

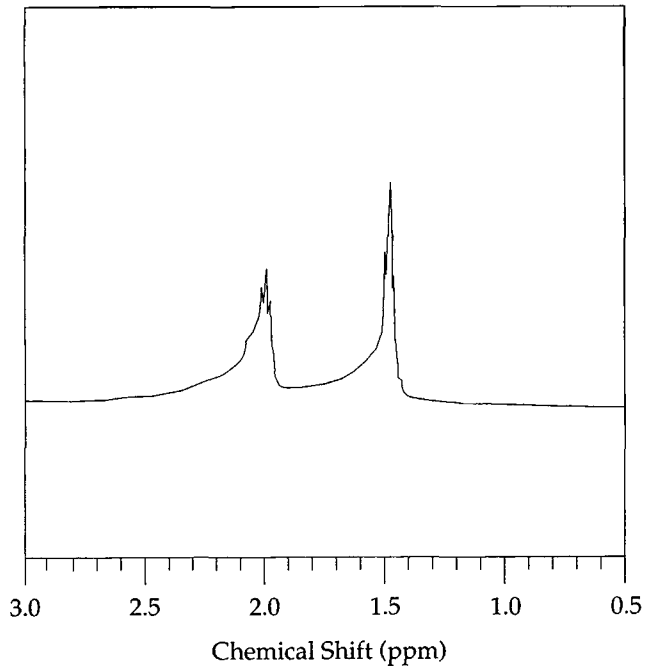

Figure 4 ^{1}H-NMR spectrum of the methine and methylene protons of the acetone-insoluble PS.

data can be determined. This method has subsequently been adopted by other authors, with modifications, and applied to similar fast-reacting systems.[11,12] It is based on the following assumptions, as outlined by Pannone and Macosko[13]:

I. Density, heat of reaction, and heat capacity of the system are constant.
II. Heat conduction through the polymer is poor, leaving adiabatic conditions at the center of the reaction mixture.
III. The reaction is sufficiently fast that heat transfer is not significant.

If these assumptions are made, then the temperature rise may be related to conversion as follows:

$$\frac{dT}{dt} = \frac{-\Delta H_r[M]_0}{\rho C_p}\frac{d\alpha}{dt} \tag{3}$$

where ΔH_r is the heat of the reaction; $[M]_0$, the initial concentration of the monomer; α, the fractional conversion; and C_p, the heat capacity of the system. The temperature of the reaction mixture, and, hence, the conversion, may then be monitored using a fast-response thermocouple connected to a data recording system.

The heat of polymerization of styrene is -69.9 kJ mol^{-1} (Ref. 14), while the heat of crystallization of polystyrene crystal is 5.8 kJ mol^{-1} (Ref. 15). The data in Table III show that the crystallinities of the samples range from 10 to 15%. The heats of crystallization of these systems range from 0.58 to 0.87 kJ mol^{-1}, which is less than 1.3% of the heat of polymerization; therefore, the effect of the heat of crystallization in the calculations was ignored.

One of the key features of the method proposed by Macosko, above, is the assumption of adiabatic behavior at the center of the system. If, however, this is not the case, heat losses from the system must be taken into account. In Lipshitz and Macosko's study,[6] reactions were conducted in a cylindrical glass container with a diameter of 38 mm. The amount of reactants used in one reaction was about 20 g. Some fine air bubbles were entrained during the mechanical mixing of the viscous liquid diisocyanate and triol. The presence of air bubbles changes the heat capacity of the material and reduces the rate of heat loss. These factors limited the heat loss to about 5% of the total heat of reaction. However, in this present s-PS work, the reactions were performed in a glass test tube with a diameter of 20 mm, and only 4 g of styrene were used in each polymerization trial. Since styrene has a low viscosity at room temperature, no fine air bubbles entrained during the mechanical mixing; therefore, the heat loss during styrene polymerization was significant, reaching levels as high as 25% of the total

Table III Summary of the Properties of the s-PS Formed at Various Conditions

No. Recipe	T_m (°C)	T_g (°C)	X_c (%)	$M_w \times 10^{-6}$	M_w/M_n	% s-PS
1	270	94	12.2	0.40	1.57	90
2	271	95	13.4	0.39	1.50	92
3	270	94	14.0	0.42	1.61	90
4	274	95	15.0	0.69	1.98	96
5	272	93	14.2	0.55	1.88	94
6	270	94	12.0	0.47	1.76	93
7	270	95	10.0	0.50	1.92	92

heat of reaction. Immediately after reaching a maximum temperature at the center of the sample plug, the temperature began to decrease at a rate of 12°C/min (as shown in Fig. 6). This is about eight times faster than Macosko's results.

One of the simplest models of heat loss involves an assumption of unsteady-state conduction.[16] If it is assumed that convective heat transfer is negligible, it has been shown that

$$\frac{d[\ln(T - T_0)]}{dt} = \beta \tag{4}$$

where β is an empirical heat-transfer coefficient, embodying the characteristics of the specific system under study. Considering small time intervals, this equation may then be manipulated to the form

$$\ln(T' - T_0) - \ln(T - T_0) = \beta(t' - t) \tag{5}$$

The change in temperature due to systemic heat loss (ΔT_{ht}) is given by eq. (6):

$$\Delta T_{ht} = -(1 - e^{\beta \Delta t})(T - T_0) \tag{6}$$

Combining eq. (3) for adiabatic internal heat generation with this equation, an equation for the change in system temperature over a short interval may be derived:

$$\Delta T = \Delta T_{hg} + \Delta T_{ht} \tag{7}$$

Table IV The Monomer Conversion of s-PS Polymerization

No. Recipe	Conversion (%) (by Mass Balance)	Conversion (%) (by TGA)
1	73	71
2	70	73
3	71	73
4	82	83
5	83	85
6	68	70
7	68	69

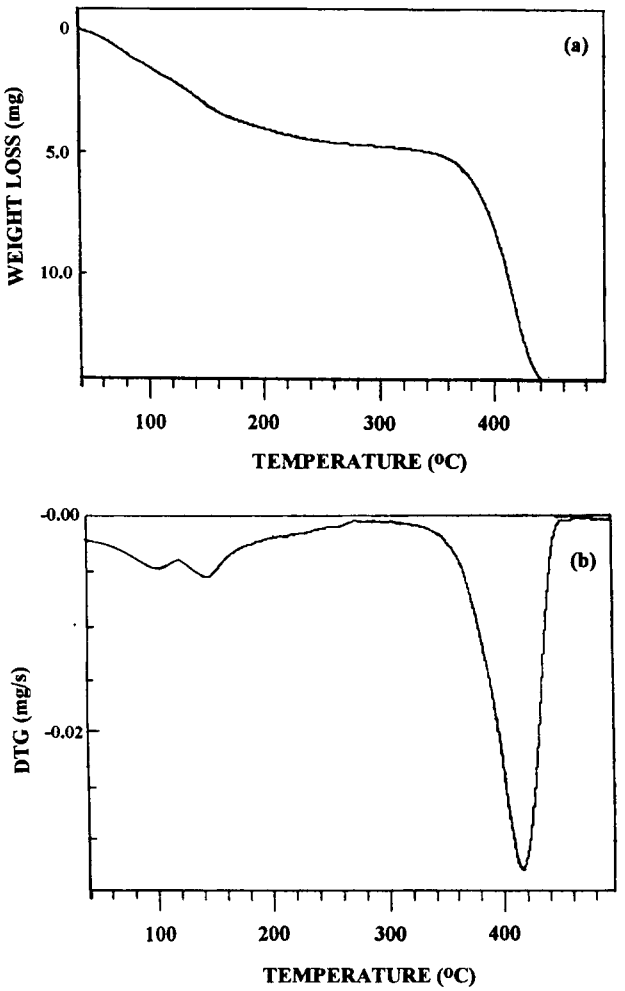

Figure 5 Thermogravimetric trace of s-PS from 30 to 500°C at a scale rate of 10°C/min: (a) the weight of sample vs. temperature; (b) the derivative of weight over time vs. temperature.

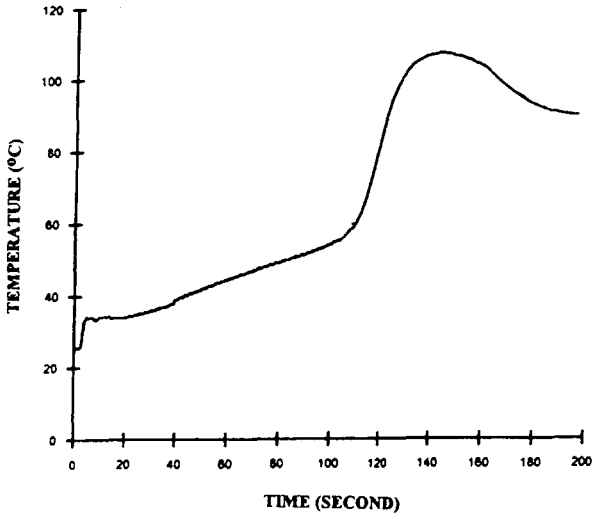

Figure 6 Temperature vs. time plot for the system with catalyst and monomer concentrations of 0.015 and 4.35 mol/L, respectively.

where ΔH_{hg} is the change in temperature due to internal heat generation, which can be calculated using eq. (3). Therefore, the total heat loss is given by eq. (8):

$$\Delta T = \frac{-\Delta H_r [M]_0 \Delta\alpha}{C_{ps}} - (1 - e^{\beta t})(T - T_0) \quad (8)$$

The value C_{ps} is an overall heat capacity for the system, assuming no loss of material due to evaporation or other means. It may be calculated based on the individual components of the system, in the case of this experiment, styrene, PS, and toluene:

$$C_{PS} = V_T \rho_T C_{P_T} + V_s \rho_s C_{P_S} \quad (9)$$

where the subscript T represents toluene and the subscript S represents the styrene phase. V is the volume of a component in the reacting system. The values of heat capacity and density of the styrene phase used are the average values for styrene and PS. Therefore, $\Delta\alpha$, corrected for heat loss from the system, may be calculated for each ΔT and Δt, yielding a plot of conversion vs. time from the experimental temperature–time data.

DISCUSSION

Analysis of the s-PS system was performed using the model stated above to correct for heat loss and obtain values of conversion with time. To obtain a value for the heat loss coefficient β, $\ln(T - T_0)$ was plotted against time. The resulting plots were all linear. Linear regression yielded slopes between -6.1×10^{-4} and -13.9×10^{-4}, and an average value of β was calculated to be -9.3×10^{-4}. Other constants used in these equations are listed in Table V.[7,14,16-18] Using these quantities, eq. (8) was applied to the temperature vs. time data to obtain corrected values of conversion vs. time. However, the corrected values predicted by the model, as it stands, only achieved a maximum of about 40%, far lower than the conversion measured by mass balance and TGA of 67–83%. On the basis of this observation, it was determined that the assumption that toluene remained in the system as a liquid was not true. Actually, the TGA trace in Figure 5(b) showed that the evaporation of toluene began at a very early stage. To obtain kinetic parameters from the data available, the heat absorbed by evaporating toluene was assumed to be proportional to the heat generated at every point, and, thus, the calculated conversions could be scaled linearly to obtain the final measured conversion. Rates of reaction were then estimated at each point of the conversion vs. temperature data by performing linear regression on the surrounding seven data points. The resulting slope can be considered to be the rate of reaction at the center point of each regression.

The temperature vs. time graph and the corrected conversion vs. time graph are shown in Figures 6 and 7, respectively. There does appear to be a sequence of distinct regimes in the overall behavior of

Table V Properties of Reactant, Solvent, and Product

Property	Value
Density of toluene, $\rho_{toluene}$	0.866 g/cm^3
Density of styrene, $\rho_{styrene}$	0.906 g/cm^3
Density of polystyrene, $\rho_{polystyrene}$	1.06 g/cm^3
Heat capacity of toluene, $(C_p)_{toluene}$	1.69 J/g K
Heat capacity of styrene, $(C_p)_{styrene}$	1.75 J/g K
Heat capacity of polystyrene, $(C_p)_{polystyrene}$	1.30 J/g K
Molecular weight of toluene, $(WM)_{toluene}$	92.13 g/g mol
Molecular weight of styrene, $(MW)_{styrene}$	104.14 g/g mol
Heat of reaction, ΔH_r	−0.670 kJ/g

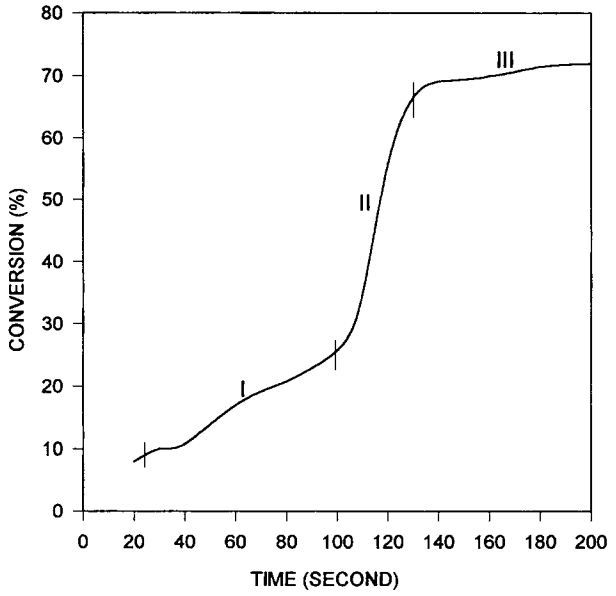

Figure 7 Monomer conversion vs. time for the system with catalyst concentration of 0.015 mol/L after heat loss correction.

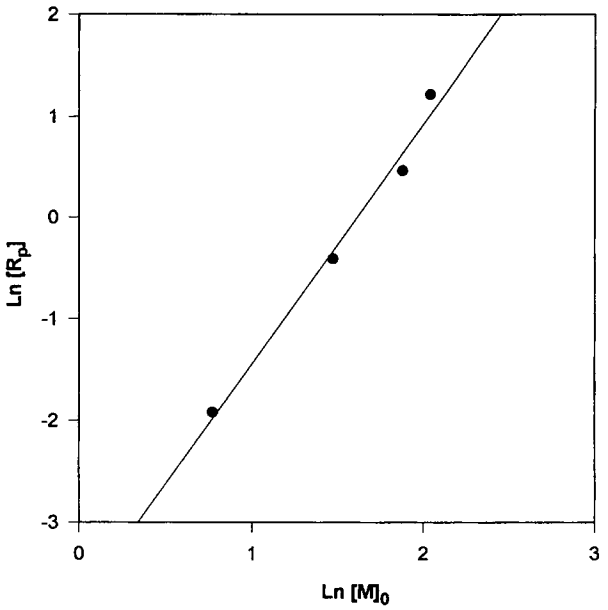

Figure 8 Van't Hoff plot for the reaction rate vs. monomer concentration.

the polymerization system. Within the first 5 s, there is a slight increase in temperature. After this initial time, the polymerization enters a period of relatively constant rate behavior, called region I. Subsequently, the polymerization enters a period of rapidly increasing rates, called region II. Finally, the rate of reaction drops to zero, as the limit of its final conversion is reached. These regions are depicted in Figure 7.

To estimate the dependency of the reaction rate on the monomer and catalyst concentrations, rates at $[M] = [M]_0$ had to be estimated. Since the behavior of the system was not uniform, and did not appear to follow a uniform rate throughout the reaction, the rate behavior in region I was considered. A period in each data set was chosen after the induction time, but before acceleration of the rate in region II. Linear regression was performed on the natural logarithm of the calculated rate against the monomer concentration in order to treat nonlinear changes in rate through this region. The initial rate was calculated for each run by substitution into the resulting linear equation.

The order of reaction with respect to monomer and catalyst concentration was determined. A Van't Hoff plot was constructed by plotting $\ln[R_p]$ vs. $\ln[M]_0$ (see Fig. 8). Here, R_p is the initial rate, and the slope of the curve is equal to the order of reaction with respect to monomer, which was found to be 2.1. Similarly, a Van't Hoff plot was constructed plotting $\ln[R_p]$ vs. $\ln[I]_0$ (see Fig. 9), and the order of reaction with respect to the catalyst was found to be close to 1.0.

Chien and Salajka[19] reported that the syndiotactic polymerization was first order in monomer concentration. The difference between our results and

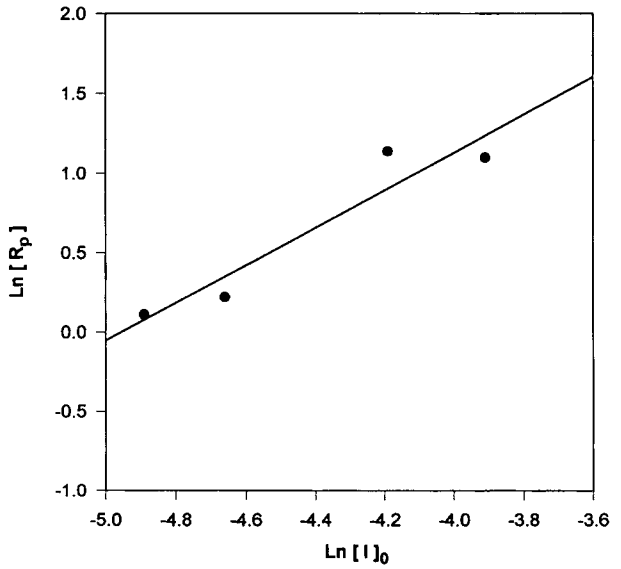

Figure 9 Van't Hoff plot for the reaction rate vs. initiator concentration.

theirs is probably caused by the different polymerization conditions. In general, the order of the reaction with respect to the catalyst has not been reported by other authors, due to the complexities involved in a catalyst/cocatalyst system. It must be noted that the values determined for the order of the reaction with respect to the catalyst and monomer were arrived at using several assumptions. On this basis, these results should be considered as a first attempt only.

The second stage of the polymerization, region II, shows an increase in the rate of polymerization beyond that achieved in region I. The autoacceleration exhibited here is similar to the Trommsdorff–Norrish effect in the free-radical bulk polymerization of poly(methyl methacrylate).[20] However, the incidence of this phenomenon in the styrene/metallocene catalyst system is uncertain. This increase in reaction rate is probably due to the rapid rise in temperature of the system. At a monomer conversion of 25%, the MW of the polymer is sufficiently high that the system begins to solidify. The additional heat of polymerization is not easily dissipated, and the temperature of the system increases significantly—hence, increasing the rate of reaction. Baird and co-workers[4] suggested that the strongly electrophilic $[Cp^*TiMe_2]^+$ may not react solely via a conventional Ziegler–Natta catalyst mechanism in styrene polymerization, but may also behave as a carbocationnic polymerization initiator. The experimental data suggest that the temperature rise has a more significant effect on chain growth than on chain termination for this system; therefore, the conversion in the region II rapidly increased.

This Cp^*TiMe_3 and $B(C_6F_5)_3$ catalyst system possesses many of the characteristics required for RIM processing. Initial solidification times, particularly at high catalyst concentrations, were significantly less than 2 min, a necessary characteristic of a successful system. Both feed components are low-viscosity fluids at room temperature, and the viscosity of the system initially remained low after mixing, permitting time to fill the mold before solidifying. Compared to many polymerization systems, the viscosity of the individual components is low enough to ensure that mixing by impingement is good.

However, there are also several potential problems associated with using this system for RIM processing. Components for RIM generally need to be stable in a tank for long periods of time. Although RIM storage tanks are generally sealed and stored under a nitrogen gas atmosphere, the vulnerability of this catalyst system to oxygen and water, even in small quantities, may be a problem. Also, the ability of uninhibited styrene to autopolymerize may cause problems during long-term storage. With respect to mold filling, it is generally necessary that the reacting mixture have a viscosity of 10–100 mPa-s. The viscosity of the components, as used currently, is outside that range. Efforts to find polymers which can be added to the monomer solution to increase its viscosity are being made, but they must not affect the catalyst. Considering the components involved in the experiments reported above, it is not desirable to use large volumes of toluene, some of which is left in the final product. The presence of toluene is confirmed, particularly at low catalyst concentrations, from the TGA data. Some preliminary work suggests that the polymerization can be carried out with the styrene monomer only. The toluene would have to be removed from the polymer prior to use of the molded part. Also, and perhaps the most critical, RIM production requires demold times of less than 3 min, or 180 s, to achieve adequate production rates. On exiting the mold, the reaction, in general, should be 95% complete. The results of these experiments show the reaction is only 68–83% complete. In short, several difficulties remain, which must be overcome prior to application of this polymer/catalyst system to RIM.

Rubber Modification

Six commercially available elastomer modifiers, identified in Table I, were investigated. Both unpurified and purified block copolymers (Kraton rubbers) were employed. The block copolymer was purified by dissolving in toluene at 70°C, followed by precipitation with methanol at ambient temperature. The rubber was then washed three times with methanol and dried to a constant weight. Three rubber concentrations of 10, 15, and 20 wt % were tested, and two methods of rubber incorporation were examined. The rubber was purged and added to anhydrous styrene or anhydrous toluene before being injected to the test tube containing the catalyst or cocatalyst, respectively.

The experimental results revealed that for Kraton rubbers only G1652 could be successfully added to the system without terminating or inhibiting the polymerization; for Kraton D1101, D1102, and D1107, no solidification of s-PS occurred. A solid plug was formed for both the unpurified and purified Kraton G 1652 at concentrations of 10 and 15 wt

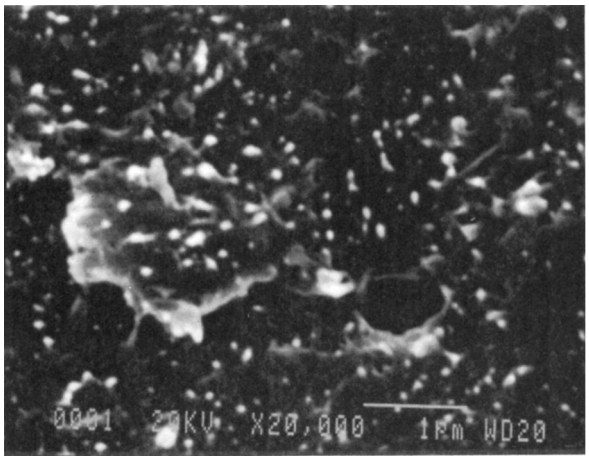

Figure 10 SEM photograph of s-PS/Kraton 1652 rubber.

%. When 20 wt % of G 1652 was added, phase separation occurred. Visually, it was easy to distinguish the white rubber from the dark PS. One reason for this phase separation could be that the rubber solution was too viscous when 20 wt % rubber was added, making mixing of the two streams more difficult. For the trial where the rubber content was 10 and 15 wt %, no phase separation was observed. The fracture surface of 15% Kraton G 1652-toughened s-PS was observed using SEM and is given in Figure 10. The average size of the dispersed phase appeared to be about 0.15 microns.

Paraloid EXL 2300 and EXL 2691 were supplied in powder form. When these rubbers were added to system, no solidification of s-PS was observed. However, for the EXL 2300, it appeared that the polymerization may have started, as the solution initially turned dark, before changing back to yellow. It is likely that there were residual reactive species on these particles which interfered with the polymerization. While only one of the elastomers could be incorporated into the reaction system without seriously retarding the polymerization, this single success suggests rubber toughening will be possible. This phase of the work further underscores how easily small amounts of contaminants can jeopardize the polymerization.

CONCLUSIONS

When styrene was polymerized to the syndiotactic polymer under conditions similar to RIM processing, conversions of 68–83% were obtained at various catalyst and monomer concentrations. Characteristic temperature vs. time plots for this system were obtained, indicating that the polymerization system passed through three distinct regions of behavior during the reaction. The adiabatic temperature rise model could not be applied directly to this system, due to substantial heat loss. The correction factors applied did not entirely account for the heat loss due to evaporation of toluene. Given a series of assumptions, however, it was found that at low conversions the reaction rate was second order in monomer and first order in catalyst. A phenomenon similar to the Trommsdorff–Norrish effect in these reactions at high conversion levels was found. A styrene ethylene–butylene styrene copolymer elastomer has been successfully added to the s-PS polymerization system.

As a potential RIM system, the styrene/$Cp^*TiMe_3/B(C_6F_5)_3$ system shows considerable promise, fulfilling many of the conditions necessary for this processing method. However, the major problems of incomplete conversion of the monomer and stability of the catalyst must be overcome before this process can be taken further.

The authors gratefully acknowledge the financial support of the National Science and Engineering Research Council. We thank Prof. K. E. Russell and Miss Betty Wong for helpful discussions.

REFERENCES

1. N. Ishihara, T. Seimiya, M. Kuramoto, and M. Uoi, *Macromolecules,* **21,** 2464 (1986).
2. W. E. Baker, V. Schytt, T. M. Liu, T. D. Jones, and M. C. Baird, in *Reactive Processing Symposium, Proceedings of the Polymer Processing Society,* Regional Meeting, Strasbourg, 1994, p. 54.
3. D. J. Gillis, M.-J. Tudoret, and M. C. Baird, *J. Am. Chem. Soc.,* **115,** 2543 (1993).
4. R. Quyoum, Q. Wang, M.-J. Tudoret, and M. C. Baird, *J. Am. Chem. Soc.,* **116,** 6435 (1994).
5. C. W. Macosko, *RIM Fundamentals of Reaction Injection Molding,* Hanser, New York, 1989.
6. S. D. Lipshitz and C. W. Macosko, *J. Appl. Polym. Sci.,* **21,** 2029 (1977).
7. *Omega Temperature Measurement Handbook and Encyclopedia,* Omega Engineering Inc., Stamford, CT, 1992.
8. J. C. W. Chien and Z. Salajka, *J. Polym. Sci. Part A Polym. Chem.,* **29,** 1243 (1991).
9. D. H. Krzystowzyk, X. Niu, R. D. Wesson, and J. R. Collier, *Polym. Bull. (Berl.),* **33,** 109 (1994).
10. R. C. West, Ed., *CRC Handbook of Chemistry and Physics,* 56th ed., CRC Press, Cleveland, 1975.

11. N. P. Vespoli and L. M. Alberino, *Polym. Proc. Eng.*, **3,** 127 (1985).
12. J.-J. A. Your, G. D. Karles, J. G. Ekerdt, I. Trachtenberg, and J. W. Barlow, *Ind. Eng. Chem. Res.*, **28,** 1456 (1989).
13. M. C. Pannone and C. W. Macosko, *Polym. Eng. Sci.*, **28,** 660 (1988).
14. J. I. Kroschwitz, Ed., *Encyclopedia of Polymer Science and Engineering,* Wiley, Toronto, 1989, Vol. 16.
15. F. de Candia, A. R. Filho, and V. Vittoria, *Colloid Polym. Sci.*, **269,** 650 (1991).
16. J. R. Welty, C. E. Wicks, and R. E. Wilson, *Fundamentals of Momentum, Heat and Mass Transfer,* Wiley, Toronto, 1984, Chap. 18.
17. S. Budavari, Ed., *The Merck Index,* 11th ed., Merck, Rahway, NJ, 1989.
18. R. E. Bolz and G. L. Tuve, Ed., *CRC Handbook of Tables for Applied Engineering Science,* 2nd ed., CRC Press, Cleveland, 1973.
19. J. C. W. Chien and Z. Salajka, *J. Polym. Sci. Part A Polym. Chem.*, **29,** 1253 (1991).
20. J. N. Cardenas and K. F. O'Driscoll, *J. Polym. Sci. Polym. Chem. Ed.*, **14,** 883 (1976).

Received February 5, 1996
Accepted May 20, 1996